Equilibrium Melting Temperature and Undercooling Dependence of the Spherulitic Growth Rate of Isotactic Polypropylene

Jiannong Xu, Srivatsan Srinivas,† and Hervé Marand*

Virginia Polytechnic Institute and State University, Department of Chemistry, Department of Materials Science and Engineering, Blacksburg, Virginia 24061-0212

Pawan Agarwal

Exxon Chemical Company, Baytown Polymer Center, Baytown, Texas 77522-5200

Received May 11, 1998; Revised Manuscript Received September 17, 1998

ABSTRACT: Studies of the temperature dependence of spherulitic growth rates, in the context of the Lauritzen−Hoffman secondary nucleation theory, and investigations of the crystallization time and temperature dependence of the melting behavior, in the context of the nonlinear Hoffman−Weeks (HW) extrapolation, are reported for isotactic polypropylene prepared with Ziegler−Natta catalysts. The quantitative agreement between estimations of the equilibrium melting temperature, T_m, through an analysis of spherulitic growth rate data and use of the nonlinear HW approach provides strong support for the latter method. The results of these studies indicate specifically that T_m (it-PP, α-phase) is in the vicinity of 212−215 °C, some 30 °C above the most commonly quoted value. This new value of the equilibrium melting temperature of it-PP leads to predictions of the crystallization temperature dependence of the initial lamellar thickness and of the correlation between the lamellar thickness and observed melting temperature, which are in good agreement with the limited morphological information available. The present studies confirm the existence of a regime II/III transition at $T_x = 139.5$ °C. The results of this study furthermore cast some doubts as to the current value of the small-angle X-ray scattering technique for the analysis of morphological parameters in quiescently crystallized isotactic polypropylene.

Introduction

In the preceding paper of this series,[1] we suggested that in the absence of isothermal lamellar thickening effects, the equilibrium melting temperature of a crystallizable polymer can be obtained through consideration of the nonlinear dependence of the observed melting temperature on the crystallization temperature. Studies to be discussed in the present paper indicate that such concepts can be successfully applied to the case of isotactic polypropylene (it-PP) synthesized with Ziegler−Natta catalysts. Specifically, our results indicate that the equilibrium melting temperature for the α-phase of it-PP derived from the nonlinear Hoffman−Weeks (HW) analysis is in good agreement with that derived from a study of the temperature dependence of isothermal spherulitic growth rates.

We specifically chose it-PP for this study for three reasons: first, there appears to be considerable discrepancies in the literature between values reported for both the equilibrium melting temperature[2−18] and the secondary nucleation constants;[7−10,20−33] second, some claims have been made[9,12] that there is agreement between the evaluation of the equilibrium melting temperature by the linear HW and the Gibbs−Thomson (GT) approaches, which, if verified, would contradict our assertion[1] that the linear HW extrapolation[34] is not justified on theoretical grounds; third, the recent synthesis of isotactic polypropylene of the controlled defect content and type, using metallocene catalysts, has led to a renewed interest in this polymer in academic and industrial circles and comparison of these polymers to their Ziegler−Natta counterpart requires the knowledge of the effect of defects on the equilibrium melting temperature.

Another important issue addressed in this manuscript is the general applicability of the Lauritzen−Hoffman (LH) secondary nucleation theory.[35,36] Although the LH concepts seem to successfully account for a large number of experimental observations in the case of linear polyethylene, criticism of the concept of regimes continues to appear in the literature.[37] It has been stated before and is important to realize that a proper test of the LH secondary nucleation theory cannot be carried out in the absence of an accurate estimate of the equilibrium melting temperature for that polymer. Critics of the regime theory have emphasized that experimentally observed regime transitions are too sharp to be associated with a change in the surface nucleation rate.[37] Such criticism can be considered meaningful only if the experimental data is evaluated with an acceptable estimate of the equilibrium melting temperature and with knowledge of the uncertainty associated with the experimental growth rates. Similarly, evaluation of secondary nucleation constants for regimes II and III and comparison of their ratio to the LH theoretical predictions[35,36] demand that the correct equilibrium melting temperature be used, as it is known that their magnitude depends sharply on the equilibrium melting temperature adopted in the analysis.

Finally, it is shown that a careful analysis of both the temperature dependence of the spherulitic growth rate and the relationship between crystallization and observed melting temperatures provides some stringent conditions on possible values for the equilibrium melting temperature, basal plane interfacial free energy, and C_2 parameter. These constraints allow one to predict

* To whom correspondence should be addressed.
† Permanent address: Exxon Chemical Company, Baytown Polymer Center, Baytown, Texas, 77522-5200.

10.1021/ma980748q CCC: $15.00
Published on Web 10/30/1998

not only the temperature dependence of the initial lamellar thickness ($l^* = C_1/\Delta T + C_2$) but also the crystallization time dependence of the average lamellar thickness, when experimental data on the evolution of the melting behavior with the crystallization time are available. Comparison of these theoretical predictions with actual experimental morphological data would then constitute a final and necessary check as to the self-consistency, if not the physical meaning, of the parameters derived from the spherulitic growth rate analysis. It is only under such conditions that secondary nucleation parameters obtained for different polymers can be compared and correlations between chain structure and crystallization behavior can be drawn.

Experimental Section

A narrow molecular weight distribution isotactic polypropylene (M_n = 41 800 g/mol, M_w/M_n = 2.09) of relatively high isotactic content (1.18% stereo defects), from the Exxon Chemical Co. was used in this study. Thin films (ca. 50 μm) were prepared by melt pressing at ca. 200 psi in a hot press at 210 °C under dry nitrogen purging and subsequent quenching in an ice−water mixture.

Prior to carrying out the isothermal crystallization studies by optical microscopy, it-PP films were melted at 200 °C for 5 min under nitrogen in a Linkam heating stage, whose temperature scale was calibrated with benzoic acid, indium, and tin. The samples were crystallized isothermally at temperatures in the range from 123 to 155 °C and the spherulitic growth was recorded using a Zeiss polarized light optical microscope equipped with a Javelin video camera and Hitachi videotape recorder. The diameter of the spherulites was recorded as a function of the crystallization time using a calibrated video caliper. As expected, the spherulite radius was observed to increase linearly with the crystallization time until impingement. Under isothermal conditions, spherulitic growth rates are then calculated from the slope of the spherulite radius versus time plots. For each crystallization temperature, an average spherulitic growth rate was estimated from a minimum of five individual experiments, each being carried out with a fresh film. The uncertainty on these average growth rates was invariably less than 5% of the magnitude of G. The spherulitic growth rates were shown to be independent of film thickness for thicknesses larger than 15 μm. The uncertainty associated with temperature fluctuations in the heating stage was estimated to be ±0.1 °C.

it-PP samples were also crystallized under isothermal conditions in the temperature range from 126 to 146 °C in a Perkin-Elmer differential scanning calorimeter model 2 operated under nitrogen flow and calibrated at different heating rates with high-purity standards from Perkin-Elmer Co. Crystallization temperatures were calibrated by extrapolation of the melting temperature of the standard to zero heating rate. The melting behavior of isothermally crystallized samples was recorded by heating these samples from their crystallization temperature up to 220 °C at a rate of 10 °C/min. The observed melting temperature was taken as the peak temperature, corrected for thermal lag.

Results

Nonlinear HW Analysis. The equilibrium melting temperature of it-PP was determined following the method described in the preceding paper in this series.[1] As was discussed in this work, for any T_m' versus T_x type analysis to be meaningful and reliable, it is imperative that the lamellar thickening coefficient be the same for samples crystallized at different temperatures. When isothermal lamellar thickening occurs, its rate increases with the crystallization temperature. However, in the usual temperature range where crystallization proceeds isothermally from the melt state, the rate of crystallization decreases with increasing temperature. It is then generally an impossible task to crystallize a given polymer over a wide range of temperatures, while ensuring a constant thickening coefficient. Rather than adjusting the crystallization time at a given temperature to control the extent of thickening, it appears more practical, at least in the case of isotactic polypropylene, to obtain the observed melting temperature of nonthickened crystals ($\gamma = 1$) by extrapolation of the melting temperature of thickened lamellae to zero crystallinity.

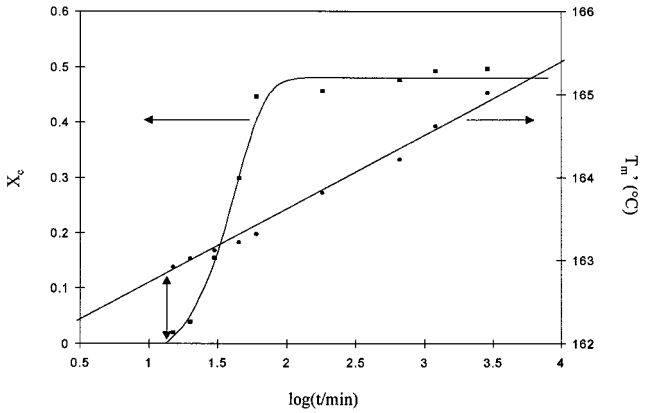

Figure 1. Evolution of the degree of crystallinity, X_c, and the observed peak melting temperature with the crystallization time at 136.0 °C.

To determine the observed melting temperature of original lamellar crystals, we follow simultaneously the evolution of the crystallinity and the observed melting temperature with time during primary crystallization at various temperatures. The melting temperature of initial lamellar crystals, T_m', is then estimated by extrapolation to the time where crystallinity is first detected. An example of the above analysis is shown in Figure 1 for T_x = 136.0 °C. The crystallinity at time t_x is determined from the heat of fusion recorded by calorimetry during a heating run initiated at T_x after crystallization for time t_x. Fitting the evolution of the crystallinity with time at early crystallization times allows one to determine t_0, the induction time at this crystallization temperature. For a given crystallization temperature, the observed melting temperature, T_m', increases linearly with the logarithm of the crystallization time during the primary crystallization stage. We can then define parameters $A(T_x)$ and $B(T_x)$ for each crystallization temperature such that

$$T_m'[T_x,t_x] = A[T_x] + B[T_x] \log[t_x] \qquad (1)$$

The observed melting temperature of original crystals at T_x is then estimated as

$$T_m'[T_x,t_0] = A[T_x] + B[T_x] \log [t_0(T_x)] \qquad (2)$$

A similar behavior for the evolution of the melting temperature with crystallization time is observed at different temperatures (Figure 2). Combining data shown in Figure 2 with the corresponding evolution of the degree of crystallinity with time allows one to derive for each crystallization temperature the parameters $A[T_x]$, $B[T_x]$, the induction $t_0(T_x)$, and $T_m'[T_x,t_0]$, the melting temperature of initial lamellar crystals at $t_0(T_x)$ (Table 1).

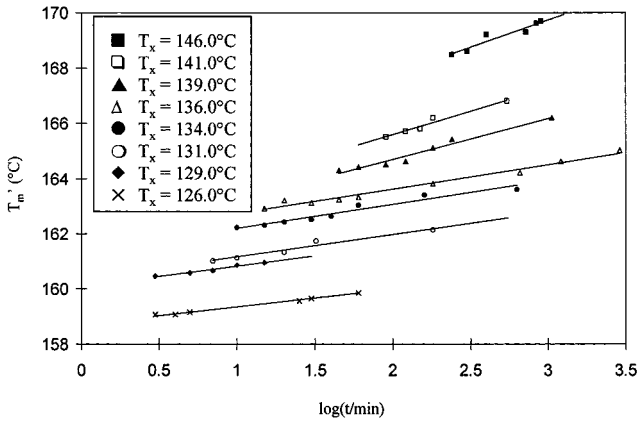

Figure 2. Evolution of the observed peak melting temperature with the crystallization time at various crystallization temperatures.

Table 1. Parameters Describing the Crystallization Time Dependence of the Observed Melting Temperature and the Induction Time for the Primary Stage of Isothermal Crystallization at Different Temperatures

T_x (°C)	$A[T_x]$ (°C)	$B[T_x]$ (°C)	$t_0(T_x)$ (min)	$T_m'[T_x,t_0]$ (°C)
126.0	158.72	0.63	0.2	158.3
129.0	160.06	0.76	1.5	160.2
131.0	160.33	0.82	4.6	160.9
134.0	161.33	0.86	7.3	162.1
136.0	161.85	0.89	11.7	162.8
139.0	161.73	1.49	27.9	163.9
141.0	162.18	1.71	36.5	164.9
146.0	163.83	1.97	50.0	167.2

We then define the quantities M and X by[1] $M = T_m/(T_m - T_m')$ and $X = T_m/(T_m - T_x)$, where T_m is the equilibrium melting temperature and T_m' is the observed melting temperature of original crystals formed at T_x. For a set of T_m',T_x values, corresponding sets of M,X values can be calculated for a given choice of the equilibrium melting temperature. We showed previously that if the initial lamellar thickness is given by $l^* = C_1/\Delta T + C_2$, where C_1 is equal to $2\sigma_e^1 T_m/\Delta H_f$ and C_2 is a constant accounting for both the term δl_x and the temperature dependence of the "kinetic" fold surface free energy, σ_{ex}, then the T_m' versus T_x relation can be rewritten as[1]

$$M = \gamma\left(\frac{\sigma_e^1}{\sigma_{em}}\right)(X + a) \qquad (3)$$

where σ_{em} is the fold surface free energy appearing in the Gibbs−Thomson equation, $a = \Delta H_f C_2/2\sigma_e^1$. We noted earlier[1] that σ_{em} may a priori differ slightly from σ_e^1. However, studies of linear polyethylene suggest that, within experimental uncertainty (ca. 5−10%), these quantities cannot be unambiguously differentiated. ΔH_f is the theoretical heat of fusion and C_2, as noted above, is a function of δl_x, the lamellar thickness increment above the minimum lamellar thickness necessary for crystal growth to proceed at a finite rate. When this method is applied to the melting of "original" crystals ($\gamma = 1$), a plot of M versus X for the "true" equilibrium melting temperature should yield a straight line of the slope unity (if $\sigma_e^1 = \sigma_{em}$) and intercept equal to a. Figure 3 shows the evolution of the M versus X plots for different choices of the equilibrium melting temperature. Figure 4 shows the variation in the slope of M versus X plots with the value adopted for the

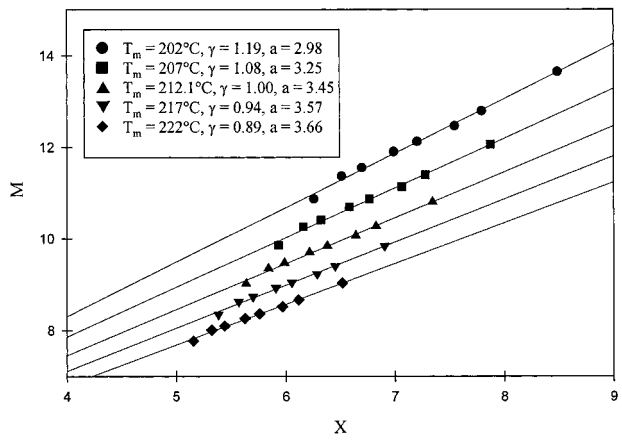

Figure 3. Plot of the scaled observed melting temperature $M = T_m/(T_m - T_m')$ versus the scaled crystallization temperature $X = T_m/(T_m - T_x)$ for various choices of the equilibrium melting temperature, T_m.

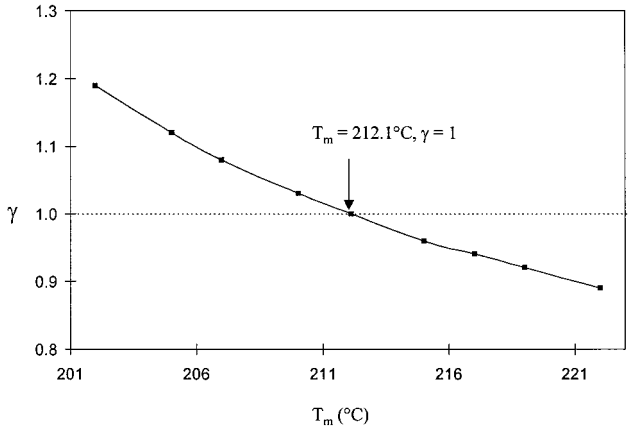

Figure 4. Plot of the thickening coefficient, γ, as a function of the chosen equilibrium melting temperature.

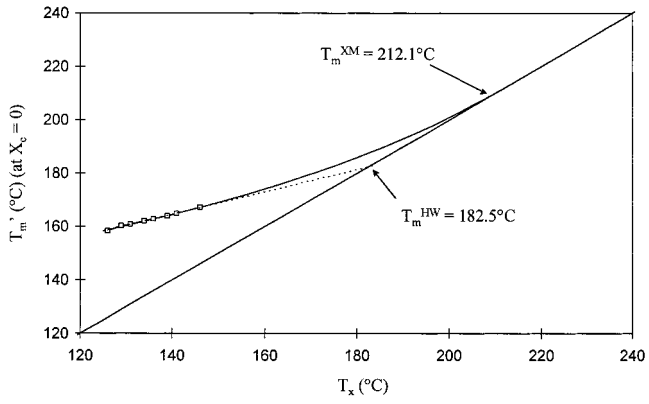

Figure 5. Plot of the observed melting temperature of initial lamellar crystals versus the crystallization temperature. The solid curve is the nonlinear HW extrapolation calculated using $a = 3.45$, $\gamma = 1$, and $T_m = 212.1$ °C. The dotted curve is the linear HW extrapolation based on experimental data points (□).

equilibrium melting temperature. The equilibrium melting temperature obtained by this method (γ =1) is found to be $T_m = 212.1$ °C. The value of a associated with this equilibrium melting temperature is then obtained from the intercept of M versus X with the M axis ($a = 3.45$). Figure 5 shows the evolution of the extrapolated melting temperature of initial crystals with the crystallization temperature. Also shown are the HW linear and nonlinear extrapolations constructed as

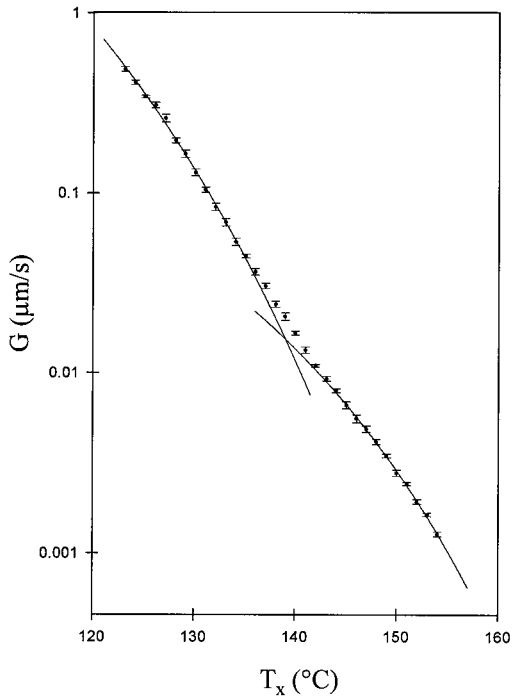

Figure 6. Plot of the experimental spherulitic growth rate versus the crystallization temperature. Error bars for the magnitude of the growth rate at each crystallization temperature are shown. The solid curves represent the theoretical expressions of G vs T_x in each regime calculated using eq 4 and data in Table 4 for $T_m = 212.1$ °C.

described previously.[1] It is quite clear that the linear and nonlinear extrapolations lead to significantly different estimates of the equilibrium melting temperature, the nonlinear estimate being higher by about 30 °C. Furthermore, the apparent thickening coefficient inferred from the linear HW analysis is estimated to be $\gamma = 2.4$, a value which is physically meaningless, as it would imply rapid and significant thickening of polymer lamellae at very short times after their formation. The constant apparent thickening coefficient suggested by the linear HW analysis[34] is furthermore inconsistent with the increase in the thickening rate with the crystallization temperature, which can be inferred from Figure 2 (data in Table 1) and from the literature.[12,38,39]

Temperature Dependence of Spherulitic Growth Rates. Spherulitic growth rates for the α-phase of it-PP measured at temperatures between 123 and 154 °C are plotted as a function of the crystallization temperature in Figure 6. A barely visible discontinuity in the temperature dependence of the curvature of ln G versus T_x is observed around 139−140 °C. This discontinuity has been observed by previous investigators in the same temperature range and has been interpreted as a II−III regime transition.[8−10,27−33] To analyze these data in the context of the Lauritzen−Hoffman secondary nucleation theory,[35,36] the growth rate is plotted as a function of the undercooling according to the classical equation:

$$\ln G_j + \frac{U^*}{R(T_x - T_\infty)} = \ln G_j^0 - \frac{K_{gj}}{T_x(T_m - T_x)} \qquad (4)$$

where U^* and T_∞ are the Vogel−Fulcher−Tamman−Hesse (VFTH) parameters describing the transport of

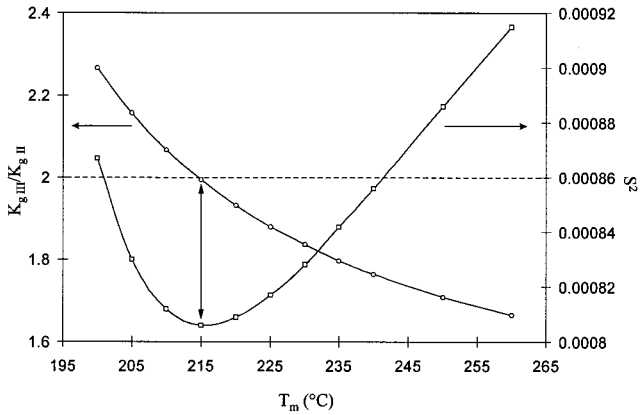

Figure 7. Ratio of secondary nucleation constants in regimes III and II, $K_{g.III}/K_{g.II}$, and overall variance of the fit, S^2, as a function of the chosen equilibrium melting temperature, T_m.

polymer segments across the liquid/crystal interphase, K_{gj} is the secondary nucleation constant in a given regime, and G_j^0 is a prefactor assumed to be independent of the temperature. Although we initially chose for the VFTH parameters the values recommended by Hoffman et al.[35,36] (i.e., $U^* = 1500$ cal/mol and $T_\infty = T_g - 30$ K), we also carried out similar analyses using different pairs of U^* and T_∞, inferred from viscoelastic measurements on at-PP melts by Plazek et al.[40] and by Pearson et al.[41] Since we do not know a priori the equilibrium melting temperature, T_m, for the α-phase of it-PP, we use a technique developed earlier for spherulitic growth studies on polypivalolactone[42,43] and calculate, for a given choice of T_m, the variance of the fit of the growth rate data to eq 4. The equilibrium melting temperature appropriate for the polymer of interest could be defined as that leading to a minimization of the variance of this fit. In the case of it-PP spherulitic growth, this process has to be carried out separately for crystallization temperatures below and above 139.5 °C to investigate the possibility of a regime II−III transition at that temperature. Furthermore, it is expected on theoretical grounds that regime transitions are not sharp but develop over some finite temperature range.[37] So, the linear regression over the experimental data is conducted in such a way as to ignore data points in the direct vicinity of the hypothetical transition (i.e., between 135 and 143 °C). Alternatively, if it is established that the polymer of interest exhibits a II/III regime transition, we could define the equilibrium melting temperature as that leading to a ratio of the secondary nucleation constants in regimes III and II equal to 2.0.[35,36] The results of these analyses (using $U^* = 1500$ cal/mol and $T_\infty = T_g - 30$ K) are shown in Figure 7 where the overall variance, S^2, and the ratio of secondary nucleation constants in the two hypothetical regimes, $K_{g.II}$ and $K_{g.III}$, are plotted as a function of the equilibrium melting temperature, T_m, chosen in the analysis. Examination of Figure 7 allows us to conclude that the best fit of experimental spherulitic growth rate data above and below $T = 139.5$ °C is obtained for a value of the equilibrium melting temperature $T_m = 215.5$ °C and that for this choice of the equilibrium melting temperature, the ratio of the two secondary nucleation constants is 1.99, in good accord with predictions from the LH theory. Alternatively, for the ratio of secondary nucleation constants to be equal to 2.0, the equilibrium melting temperature should be 214.5 °C. The results of similar analyses carried out with different

Table 2. Equilibrium Melting Temperature and Secondary Nucleation Constants Determined through the Analysis of the Temperature Dependence of the Spherulitic Growth Rate Assuming Specific Values of U^* and T_∞ and Specific Criteria (A−D; See Text)

criteria	U^* (cal/mol) T_∞ (K)	0	1500[27] 231.2[27]	2043[40] 233.2[40]	2684[41] 224.2[41]	2932[40] 213.2[40]
A	T_m (°C)	212.6	223.6	228.4	231.5	230.8
	$10^{-5}K_{g.II}$ (K^2)	3.60	5.70	6.82	7.63	7.46
	$10^{-5}K_{g.III}$ (K^2)	7.23	10.8	12.7	14.0	13.7
	$K_{g.III}/K_{g.II}$	2.00	1.89	1.86	1.83	1.83
B	T_m (°C)	196.6	209.2	214.9	218.3	217.1
	$10^{-5}K_{g.II}$ (K^2)	1.92	3.56	4.51	5.18	4.97
	$10^{-5}K_{g.III}$ (K^2)	4.49	7.40	9.03	10.14	9.78
	$K_{g.III}/K_{g.II}$	2.34	2.08	2.00	1.96	1.97
C	T_m (°C)	204.0	215.5	220.6	223.9	222.9
	$10^{-5}K_{g.II}$ (K^2)	2.62	4.42	5.42	6.15	5.95
	$10^{-5}K_{g.III}$ (K^2)	5.66	8.79	10.5	11.7	11.3
	$K_{g.III}/K_{g.II}$	2.16	1.99	1.93	1.90	1.90
D	T_m (°C)	213.1	214.5	215.1	215.2	214.7
	$10^{-5}K_{g.II}$ (K^2)	3.66	4.28	4.54	4.68	4.59
	$10-5K_{g.III}$ (K^2)	7.33	8.56	9.08	9.36	9.18
	$K_{g.III}/K_{g.II}$	2.00	2.00	2.00	2.00	2.00

Table 3. Secondary Nucleation Constants and Basal Plane Interfacial Free Energy Determined through the Analysis of the Temperature Dependence of the Spherulitic Growth Rate Assuming $U^* = 1500$ cal/mol, $T_\infty = T_g - 30$ K and Different Values of T_m

	$T_m = 185$ °C	$T_m = 212.1$ °C
$10^{-5}K_{g.II}$ (K^2)	1.01	3.94 ± 0.41
$10^{-5}K_{g.III}$ (K^2)	3.02	8.03 ± 0.67
$K_{g.III}/K_{g.II}$	2.99	2.04 ± 0.05
σ_e^1 (erg·cm^{-2})[a]	49.1	146 ± 44

[a] We assumed a (110) growth plane[67] and took σ as the average of values obtained through the Thomas−Staveley empirical equation[49] ($\sigma_{TS} = 11.3$ erg·cm^{-2}) and through the $\sigma-C_\infty$ correlation[50] ($\sigma_{C_\infty} = 12.6$ erg·cm^{-2}). The uncertainties are calculated conservatively assuming separate uncertainties of ±3 °C on T_m and ±2 erg·cm^{-2} on σ.

sets of U^* and T_∞ are given in Table 2. In this table, we give the values of T_m, $K_{g.II}$, $K_{g.III}$, and $K_{g.III}/K_{g.II}$ determined using four different criteria (A−D). For criterion A, the "best" equilibrium melting temperature is that leading to the minimization of the variance in regime II. Similarly, criterion B defines the best choice of T_m from the minimization of the variance in regime III. Criterion C uses a minimization of the overall variance (sum of variances in regimes II and III) to define the best T_m, whereas criterion D determines T_m as the value leading to a ratio of 2 for the secondary nucleation constants in regime III and II. We have also analyzed the temperature dependence of spherulitic growth rates using $U^* = 1500$ cal/mol and $T_\infty = T_g - 30$ K and assuming either $T_m = 185$ °C, the most widely reported equilibrium temperature for the α-phase it-PP[2−12,27], or $T_m = 212.1$ °C, the equilibrium melting temperature predicted by the nonlinear HW analysis. The results of these analyses are given in Table 3. Plots of $\ln G + U^*/R(T - T_\infty)$ versus $1/T\Delta T$ for $T_m = 212.1$ and $T_m = 185$ °C are shown in Figures 8 and 9, respectively. Note that, in both cases, the data "appear" to be linearized. However, if one calculates the difference between the experimental values of $\ln G + U^*/R(T - T_\infty)$ and the calculated values of $\ln G_j^0 - K_{gj}/T\Delta T$ for both $T_m = 212.1$ and 185 °C, systematic deviations are observed between fitted and experimental values only for the lower equilibrium melting temperature (Figures 10 and 11, respectively). This is a clear indication that the curvature of ln G versus T is accounted for much better by choosing $T_m = 212.1$ °C as the appropriate equilibrium melting temperature for this polymer. Examination of Figures 6 and 8 suggests that the transition between regimes II and III for it-PP occurs gradually over a temperature range of approximately 9 °C. The criticism[37] that the observed II/III regime transition is too sharp is therefore not supported by our study.

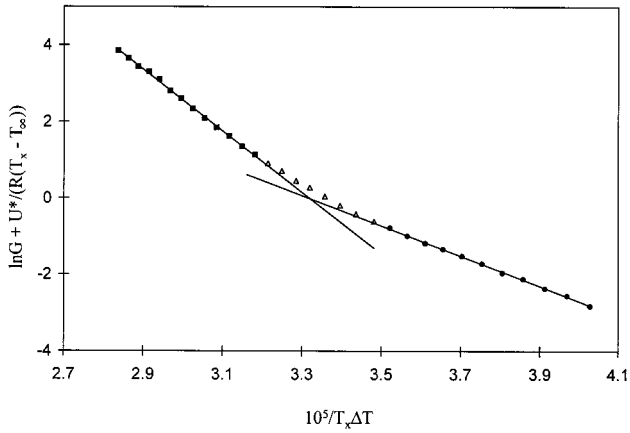

Figure 8. LH plot for $T_m = 212.1$ °C, $U^* = 1500$ cal·mol^{-1}, and $T_\infty = T_g - 30$ K. Regime III data used in the analysis (■). Regime II data used in the analysis (●). Data in the transition region ignored in the analysis (△).

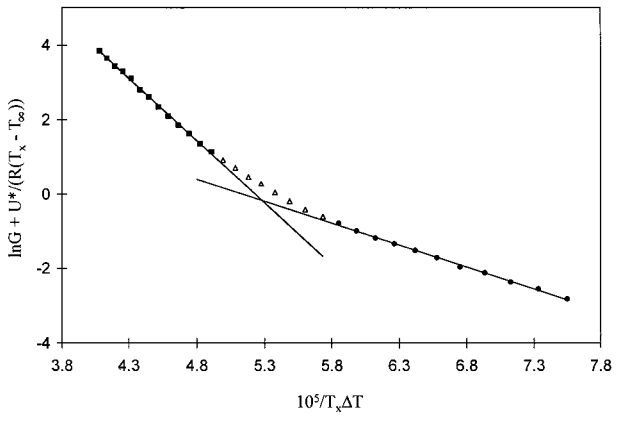

Figure 9. LH plot for $T_m = 185$ °C, $U^* = 1500$ cal·mol^{-1}, and $T_\infty = T_g - 30$ K. Regime III data used in the analysis (■). Regime II data used in the analysis (●). Data in the transition region ignored in the analysis (△).

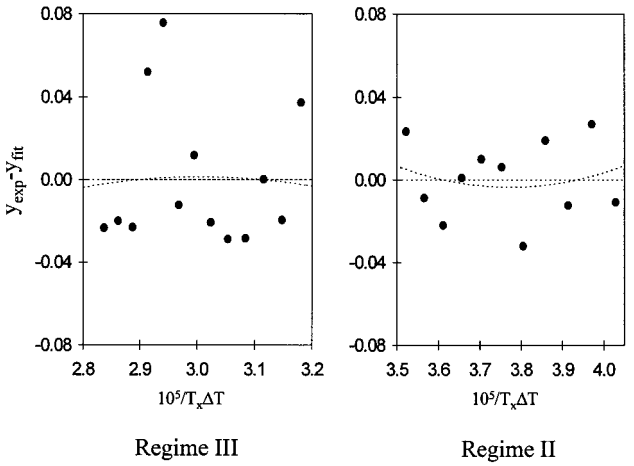

Figure 10. Difference between experimental and fitted spherulitic growth rates as a function of $1/T_x\Delta T$ for regimes II and III for LH plot based on $T_m = 212.1$ °C.

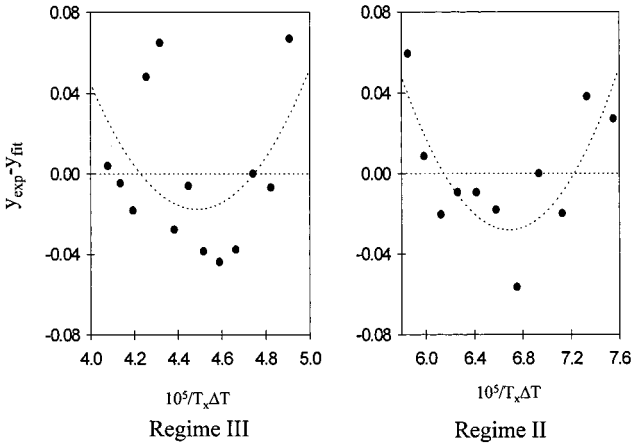

Figure 11. Difference between experimental and fitted spherulitic growth rates as a function of $1/T_x\Delta T$ for regimes II and III for LH plot based on $T_m = 185$ °C.

Discussion

Analysis of the Temperature Dependence of Spherulitic Growth Rates. The second method used in this manuscript for estimation of the equilibrium melting temperature of α-phase it-PP was used successfully in previous crystallization studies of polypivalolactone and blends of polypivalolactone with vinylidene fluoride homo- and copolymers.[42−44] This method is based on the assumption that the spherulitic growth rate, G, of high enough molecular weight polymers (i.e., nonoligomeric) can be well-represented far above the glass-transition temperature by the expression $\ln G \propto 1/T\Delta T$, where ΔT is the undercooling ($T_m - T_x$) below the equilibrium melting temperature. A reliable estimate of T_m can then be obtained through linearization and refinement of the fit of experimental G data using results of secondary nucleation theories. As long as the analysis is restricted to growth rate data obtained on the right-hand side of the G versus T curve, the estimate thereby obtained should be fairly independent of the choice of the functional form or specific parameters used to describe the effect of chain transport on the crystal growth rate. Examination of Table 2 indicates that, regardless of the choice of the U^*,T_∞ pair used in the analysis, the equilibrium melting temperature is always significantly higher than 185 °C and more likely in the vicinity of 215 °C. The best results (i.e., these simultaneously yielding the lowest value of S^2 and a ratio of $K_{g.III}$ to $K_{g.II}$ equal to 2.0) are obtained when the values $U^* = 1500$ cal/mol and $T_\infty = T_g - 30$ K are used. One should ascertain whether this result is an indication that the segmental dynamics in the direct vicinity of a crystal growth front indeed differs from that in the bulk melt or whether the LH secondary nucleation theory is only capable of capturing the essential features of the growth kinetics at low undercoolings, where the supercooled melt is not too far from equilibrium. Incidentally, at low undercoolings, the kinetics of the crystal growth process is largely dominated by secondary nucleation effects and independent of the details associated with the segmental dynamics. Although this should not be a surprise to those who use the LH theory, the classical growth rate expression (eq 4) is actually the result of a number of approximations that are only justifiable at low undercoolings. Indeed, the major goal of Hoffman and co-workers has been to provide a physically meaningful account of linear polyethylene crystallization (i.e., at undercoolings less than 30 K).[36] Although an exhaustive listing of the assumptions necessary to reach eq 4 is beyond the scope of this manuscript, the reader is reminded that the LH theory assumes, for the sake of mathematical tractability, that the segmental dynamics associated with first stem deposition is identical to that associated with subsequent stem depositions. That this is inadequate can be anticipated by stating that first stem deposition is viewed as a local segmental process (Rouse-like), while substrate completion may involve significant reeling in effects and therefore the friction coefficient of a whole chain (for chain lengths low enough that multiple pinning at different sites is not likely).[45,46] Second, and more closely related to the choice of the specific values to be used for U^* and T_∞, the friction coefficient used in the transport term, β, should be viewed as an apparent friction coefficient and not as the true friction coefficient associated with the reptative motion of polymer chains in an equilibrium melt. As was discussed in previous manuscripts,[45,46] the friction coefficient, which is defined through the equality between the nucleation-based substrate completion rate and the forced-reptation-based substrate completion rate, must also reflect the multitude of unsuccessful conformational transitions involved in the process of chain folding. As was alluded to in that work, the apparent friction coefficient may be a complicated function of the apportionment factors for first and subsequent stem placement and of the work of chain folding. One should therefore not expect a priori to obtain the best fit of the temperature dependence of crystal growth rates by simply combining the "secondary nucleation" exponential with the Vogel or Arrhenius transport term obtained from viscoelastic studies of the bulk melt. This should be especially true at large undercoolings near and below the growth rate maximum, where the segmental dynamics becomes more important. It was actually shown in the case of isotactic polystyrene, which can be crystallized isothermally at temperatures in the vicinity of the glass transition, that consideration of a third exponential term, involving the work of chain folding, allows one to reconcile the values of the Vogel−Fulcher−Tamman−Hesse parameters obtained from growth rate and viscoelastic measurements.[47,48] Such an approach cannot, however, be rigorously attempted here since growth rate

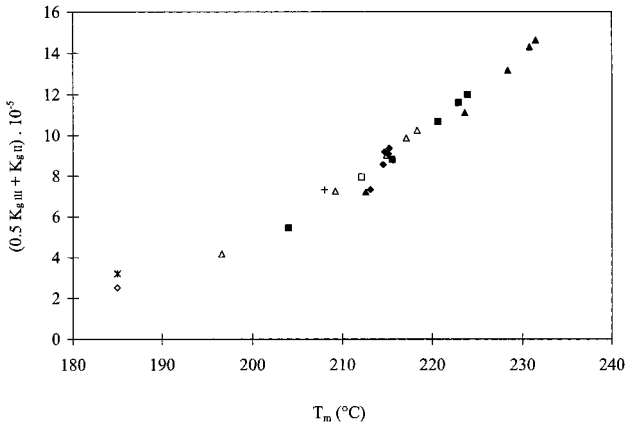

Figure 12. Average secondary nucleation constant ($0.5K_{g.III} + K_{g.II}$) versus the equilibrium melting temperature, T_m, chosen in the LH analysis. (■) This work for the global minimum of S^2; (▲) this work for the minimum of S^2 in regime II; (△) this work for the minimum of S^2 in regime III; (◆) this work for $K_{g.III}/K_{g.II} = 2$; (∗) Cheng et al.;[9] (+) Monasse et al.;[8] (◇) this work for $T_m = 185$ °C; (□) this work for $T_m = 212.1$ °C.

Table 4. Thermodynamic and Crystallographic Parameters for the Monoclinic α-Crystal Phase of it-PP

		ref no., comments
ΔH_f (J/g)	207	ref 81
ρ_c (g/cm^3)	0.934	ref 75
a_0 (cm)	5.49×10^{-8}	ref 57, assuming (110) growth front[67]
b_0 (cm)	6.26×10^{-8}	ref 57, assuming (110) growth front[67]

measurements are only available on the high-temperature side of the growth rate curve for it-PP.

With this proviso in mind, we can nevertheless state that the equilibrium melting temperature derived from the nonlinear HW analysis is consistent with that obtained through the growth rate analysis, when $U^* = 1500$ cal/mol and $T_\infty = T_g - 30$ K. It is also comforting to note in Table 2 that the ratio of the secondary nucleation constants in regimes II and III does not depend significantly on the choice of U^* and T_∞. Examination of Table 2 further shows that, although the equilibrium melting temperature predicted by the analysis of spherulitic growth rates is significantly higher than the currently accepted value of 185 °C, variation in the parameters U^* and T_∞ may lead to a somewhat significant uncertainty in the value of T_m, when variance-based criteria are used. These results further indicate that different equilibrium melting temperatures are predicted, depending on which regime is considered in the minimization of the variance. Although resolution of this issue must await (1) a better understanding of the exact temperature dependence of segmental dynamics during crystallization (see above) and (2) a more rigorous extension of eq 4 for high undercoolings, it appears, at least for it-PP, that criterion $D(K_{g.III}/K_{g.II} = 2)$ leads to a much narrower spread in the estimated T_m value. Obviously, use of this criterion relies on the assumption that regime transition concepts are physically meaningful.

Examination of Tables 2 and 3 also allows us to confirm the earlier statement that reliable secondary nucleation constants can only be obtained if the estimate of the equilibrium melting temperature is sufficiently accurate. In Figure 12, the average secondary nucleation constant ($0.5K_{g.III} + K_{g.II}$) is plotted as a function of the equilibrium melting temperature (data from Tables 3 and 4). A clear correlation between the equilibrium melting temperature chosen for the analysis and the resulting secondary nucleation constant derived from the LH plot can be observed. Note the large difference between nucleation constants for the lowest T_m values (182.8 and 185 °C) and for the T_m value extracted from the nonlinear HW analysis ($T_m = 212.1$ °C).

Knowledge of the secondary nucleation constants $K_{g.II}$ and $K_{g.III}$ (see Table 3) and of the various thermodynamic and crystallographic parameters for it-PP (Table 4) enables the determination of the magnitude of the basal plane interfacial free energy, σ_e^1, if the lateral melt/crystal interfacial free energy, σ, is known. This latter quantity can be calculated either from the Thomas−Staveley equation[49] ($\sigma_{TS} = 11.3$ erg·cm^{-2}) or from the recently proposed correlation between σ and C_∞, the chain characteristic ratio ($\sigma_{C_\infty} = 12.6$ erg·cm^{-2}).[50] Taking the average of these two values for σ, we determine $\sigma_e^1 = 146$ erg·cm^{-2}.

Correlations between Crystallization Temperature, Melting Temperature, and Lamellar Thickness. Using the value obtained for σ_e^1, we can now obtain an estimate of the C_2 parameter for α-phase it-PP from the intercept a of the M versus X plot shown in Figure 3 for $\gamma = 1$. Assuming $T_m = 212.1$ °C, the value obtained for it-PP is $C_2 = 52$ Å, which appears reasonable, when considered in light of that estimated for linear polyethylene (C_2(PE) = 43 Å).[1] Note that the value of C_2 so estimated is larger than δl_x calculated using the LH theory with $\psi = 0$ ($\delta l_x = 6$ Å), a result which was discussed previously in the case of linear polyethylene.[1] Knowledge of σ_e^1, C_2 and of the theoretical enthalpy of fusion of α-phase it-PP (Table 4) further enables the estimation of the temperature dependence of the initial lamellar thickness for it-PP.

$$l^* = \frac{7342}{212.1 - T_x} + 52 \qquad (5)$$

where l^* is given in Å and T_x in °C. The accuracy of this relationship is dependent on the validity of our assumption that σ is appropriately given either by the Thomas−Staveley empirical equation or by the $C_\infty - \sigma$ correlation, since the magnitude of σ_e^1 (146 erg·cm^{-2}) was calculated from the ratio of $\sigma\sigma_e^1$ (derived from K_g's) to that of σ. Furthermore, one must bear in mind that the accuracy of the proposed relationship depends on our ability to extract the melting temperature associated with the initial lamellar thickness through an extrapolation to short times of the melting temperature of annealed crystals. Finally, this relationship only pertains to the thickness of the leading radial lamellae and not to the subsidiary lamellae which nucleate epitaxially, initially on leading lamellae and subsequently on daughter lamellae and which give rise to the well-documented cross-hatched morphology.[51−58]

Having established new values for the equilibrium melting temperature, the C_2 parameter, and the basal plane interfacial free energy for the α-phase of it-PP, we can now discuss the extent of lamellar thickening to be expected for isothermally crystallized it-PP. Equation 5, above, provides an estimate of the undercooling dependence of the initial lamellar thickness, l^*. The Gibbs−Thomson equation[35] (eq 6, below), on the other

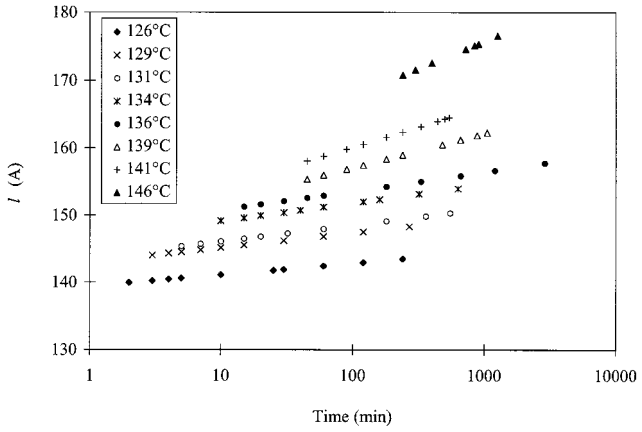

Figure 13. Estimated lamellar thickness as a function of the crystallization time and temperature. Calculation based on T_m = 212.1 °C, C_2 = 52 Å, σ_e = 146 erg·cm^{-2}, and ΔH_f = 193 J·cm^{-3}.

hand, yields a relationship between the observed melting temperature and lamellar thickness, l:

$$T_m' = T_m\left(1 - \frac{2\sigma_{em}}{\Delta H_f l}\right) \tag{6}$$

Combination of eqs 5 and 6 with the definition of the thickening coefficient $\gamma = l/l^*$ allows us to predict the crystallization time and temperature dependences of the thickening coefficient and the lamellar thickness:

$$\gamma(t) = \frac{l(t)}{l^*} = \frac{\dfrac{2\sigma_{em}T_m}{\Delta H_f(T_m - T_m')}}{\dfrac{2\sigma_e^1 T_m}{\Delta H_f(T_m - T_x)} + C_2} = \left(\frac{\sigma_{em}}{\sigma_e^1}\right)\frac{M(t)}{(X + a)} \cong \frac{M(t)}{(X + a)} \tag{7}$$

From the data presented in Figure 2, we can then prepare the plot of $l(t)$ shown in Figure 13. This plot clearly suggests that the thickening coefficient for the α-phase of it-PP increases with the crystallization temperature but remains very minimal in the temperature range investigated. The predicted lamellar thicknesses range from 145 Å at 126 °C to nearly 165 Å at 141 °C for a crystallization time of approximately 4 h. These predictions are in relative good agreement, especially at low crystallization temperatures, with recent morphological studies by White et al.[57] It is also worth noting that an increase in the thickening rate is observed at the onset of regime II. This is obviously expected from a higher probability for adjacent reentry folding in regime II than in regime III.[36] A similar conclusion was reached by Mezghani et al.[12] Lamellar thickening for it-PP is certainly expected on the basis of the existence of a crystal α-relaxation[59−62] for this polymer, relaxation associated with helical jump motions in the crystal phase, which allows a net transport of segments from the metastable amorphous fraction into the more stable crystal phase. We speculate that the small extent of lamellar thickening estimated for it-PP, as compared to that of polyethylene, may be related to the combination of a significantly higher activation energy for the α-relaxation of it-PP,[59−63] and the crystallization in regimes III and II for it-PP as opposed to that of II and I for PE. Raising the crystallization temperature of PE through the II/I regime transition has already been shown to lead to a significant enhancement in the rate of lamellar thickening.[36]

Self-Consistency of the Analysis and Comparison with Previous Results. At this juncture, it is worth comparing the results presented in this manuscript with those from previous investigations. We will first address the evaluation of the equilibrium melting temperature through the linear HW and the GT analyses. The discussion will obviously be restricted to the analysis of the thermodynamic parameters describing the crystal growth and melting processes for the α-phase of it-PP.

Equilibrium melting temperatures obtained by the HW linear extrapolation generally fall into two widely different ranges 185−190 °C[2−12] and 208−220 °C.[4,8,13−19] Certainly a range of equilibrium melting temperatures is expected a priori on the basis of tacticity and molecular weight differences between samples studied.[9,10] Furthermore, recent studies by VanderHart et al.[64] indicate that different defect types are included to different extents in it-PP α-phase crystals. Specifically, the regio defects found in metallocene-based isotactic polypropylene are thought to be for the most part excluded from the lamellar structures (ca. 10% inclusion), whereas the stereo defects found in both metallocene and Ziegler−Natta it-PP are much more significantly incorporated (ca. 50−60% inclusion). The level of defect incorporation may obviously also depend on crystallization temperature (the lower the undercooling, the lower the expected level of defect inclusion). The fact that stereo defects can be at least partially included in the lamellar crystals furthermore provides some justification for our use of the Gibbs−Thomson and LH theories for it-PP. It is noted that such theories should not rigorously apply for statistical copolymers or steroirregular homopolymers where defects are not included in the crystalline lattice, since, in these cases, the average lamellar thickness is not solely controlled by the undercooling but is also strongly influenced by the defect distribution along the polymer backbone.

Since most of the early studies focused on Ziegler−Natta it-PP but did not report the tacticity of the materials investigated, we only consider the two most recent studies by Cheng et al.[9] and Mezghani et al.[12] where the stereo defect content was less than 1%. Clearly, for these latter materials, the highest possible value of the equilibrium melting temperature for the α-phase of it-PP should be obtained. Both studies concluded through a combination of linear HW extrapolation and the GT analysis that the equilibrium melting temperature in the high chain length limit should be ca. 185 °C. In the above studies, the observed melting temperature used in the linear HW analyses was either that recorded visually at the disappearance of a birefringence of very small spherulites during heating in an optical microscope hot stage[12] or that taken as the onset of the melting endotherm.[9] Examination of results obtained in our study confirms that, indeed, a linear extrapolation of T_m' versus T_x in the limit of very short crystallization times yields a similar value for the apparent equilibrium melting temperature. We have, however, established[1] that such a linear extrapolation is without physical basis and that the extrapolation must indeed be nonlinear, if it is to be consistent with the theory it is based on. Furthermore, from the

examination of the T_m' versus T_x data from Mezghani et al.,[12] we can infer that the apparent thickening coefficient (reciprocal of the slope of the T_m' versus T_x regression) is in the range 2.4−2.7, even for samples that were crystallized for extremely short times at crystallization temperatures in the range 116−145 °C. The thickening coefficient inferred from samples crystallized for short times is actually predicted to be higher than that for samples crystallized for long times. Such a value of the apparent thickening coefficient is clearly inconsistent with the expectation of insignificant isothermal lamellar thickening in very small spherulites and with an increase in the magnitude of γ with the crystallization time and temperature. Further examination of these data confirms our prediction[1] that as the range of crystallization temperatures where the linear extrapolation is carried out is shifted down, the linearly extrapolated value of the apparent equilibrium melting temperature is more significantly underestimated ($T_m^{app} = 184.5$ °C for T_x in the range 116−136 °C versus $T_m^{app} = 188.5$ °C for T_x in the range 126−145 °C). In this work,[12] the linear extrapolation of the observed melting temperature versus the crystallization temperature data for impinged spherulites leads to an apparent equilibrium melting temperature of 210.1 °C. The situation appears here very similar to that discussed in the preceding paper[1] for the melting of linear polyethylene. An apparently correct value of the equilibrium melting temperature is obtained for fortuitous reasons associated with the effect of the crystallization temperature and crystallization time on the magnitude of the thickening coefficient. The larger scatter in the data for long crystallization times than for short ones is again a hint that samples crystallized at different temperatures and for different durations exhibit a nonconstant thickening coefficient. Similar conclusions can be drawn from the data published by Cheng et al.[9]

We now turn our attention to the Gibbs−Thomson analyses of it-PP published in the literature and specifically to these by Cheng et al.[9] and Mezghani et al.[12] which appear to present the most complete data sets. In all cases, the G−T analysis was carried out through a combination of differential scanning calorimetry to measure observed melting temperatures and small-angle X-ray scattering to estimate lamellar thicknesses. In one case,[9] the lamellar thickness was obtained at the crystallization temperature using the correlation function approach, whereas in the other case,[12] it was estimated at room temperature from the Lorentz corrected long period and the bulk crystallinity measured through wide-angle X-ray diffraction. Plots of T_m' versus $1/l$ are then constructed to obtain the equilibrium melting temperature from the intercept at $1/l = 0$ and the basal plane interfacial free energy, σ_e, from the slope. Focusing first on Mezghani et al.'s data,[12] the equilibrium melting temperature is found to be 186.1 °C in good agreement with the values of 184.5 and 188.8 °C obtained from the linear HW analysis. The magnitude of σ_e was not reported but can be estimated to be 45 erg·cm^{-2}, if a value of 193 J/cm^3 is used for the theoretical heat of fusion. From this value of the fold interfacial free energy, one can infer a work of chain folding, $q = 4.4$ kcal/mol, if a (110) growth plane is assumed. Turning now to Cheng et al.'s data,[9] the inferred equilibrium melting temperature is 185 °C, again in agreement with the linear HW extrapolation. The fold interfacial free energy value is calculated to be 31 erg·cm^{-2}, leading to a work of chain folding, $q =$ 3 kcal/mol. The values reported above for the work of chain folding are obviously significantly different from one another (ca. 50%), but more surprisingly, are lower than that of linear polyethylene ($q = 4.9$ kcal/mol).[36] Furthermore, these values appear to be inconsistent with those obtained from the analysis of the temperature dependence of spherulitic growth rates (52−70 erg·cm^{-2})[9,27] when one assumes $T_m = 185$ °C and $\sigma =$ 11.5 erg·cm^{-2}. We recall the results shown in Figure 12 and the observation made earlier by Monasse et al.,[8] that choosing a higher equilibrium melting temperature leads to a larger estimate of the fold surface free energy. From the secondary nucleation constants given by Monasse et al.[8] and the thermodynamic and crystallographic parameters shown in Table 4, σ_e^1 is estimated to be 141 erg·cm^{-2} ($q = 13.9$ kcal/mol), consistent with our own results.

Having addressed above and in the preceding paper[1] the reasons for the lack of applicability of the linear HW extrapolation, we must now discuss why the Gibbs−Thomson analysis also generally leads to erroneous results in the case of it-PP. To shed some light on this issue, it is worth examining again Mezghani et al.[12] and Cheng et al.[9] SAXS data. From the Gibbs−Thomson plots published by these authors, we can determine the range of lamellar thicknesses and observed melting temperatures investigated. In the former study,[12] calculated lamellar thicknesses range from 98 Å ($T_m' =$ 164 °C) to 166 Å ($T_m' = 173.5$ °C), whereas in the latter study,[9] they range from 27 Å ($T_m' = 131.9$ °C) to 98 Å ($T_m' = 171.9$ °C). Some inconsistency between these two data sets is already apparent in the fact that for it-PP samples of similar stereo defect content (less than 1%) and of identical lamellar thickness (98 Å) a difference of 8 °C in the observed melting temperature is reported. This discrepancy cannot be explained by differences in the definition adopted for the melting temperature (the endotherm peak in one case[12] and the endothermic peak onset in the other case[9]) and is inconsistent with the observation that both studies yield the same extrapolated equilibrium melting temperature. One could argue that the correlation function approach cannot be employed to analyze SAXS data for it-PP after cooling below the isothermal crystallization temperature. According to Strobl et al.,[65] the lack of applicability of the correlation function approach stems from the significant increase in crystallinity observed during cooling, the associated change in the specific inner surface, and the departure of the morphology from the lamellar stack model. Indeed, in one case,[9] lamellar thicknesses were estimated using the correlation function approach with scattering data recorded at each crystallization temperature, whereas in the second case,[12] they were determined at room temperature by multiplying the Lorentz-corrected long period, L_B, by the WAXD crystallinity, X_c^W. Strobl et al.[65] point out that the significant increase in crystallinity observed in it-PP upon cooling below the crystallization temperature is not accompanied by a change in long spacing. One would therefore expect that the it-PP lamellar thickness estimated through a combination of room-temperature SAXS and WAXD measurements are overestimated. This conclusion is, however, neither supported by a comparison of the two sets of SAXS/DSC data[9,12] nor is it supported by comparison of SAXS[9,12] and TEM[57] data.

To show the general failure of the SAXS technique to provide reliable morphological details for isotactic polypropylene, we will briefly review the pertinent literature. First, it is established that when it-PP crystallizes in the form of α-phase spherulites, the spherulites exhibit a birefringence whose sign and magnitude depend on crystallization temperature.[53,55] The birefringence continuously decreases from positive values at low crystallization temperatures to negative values at higher temperatures. The temperature where the change in the birefringence sign is observed is dependent on molecular weight and on the content in stereo and other defects along the chains. Second, it is equally well-established that the change in spherulite birefringence with the crystallization temperature is associated with the corresponding change in the relative fraction of radial and nearly tangential lamellae within the spherulites.[51−53,55] Following the nomenclature of Bassett,[57] the dominant lamellae within the spherulites are obviously always radial but subsidiary lamellae can be either radial or tangential. Tangential lamellae are initiated by homoepitaxy on radial lamellae and subsidiary radial lamellae are initiated by similar epitaxy on tangential lamellae. This crystallographic lamellar branching, apparently unique to the α-phase of it-PP, is triggered by the similarity in the unit cell a and c axis dimensions and the presence of helices of the same hand in two successive ac layers of the parent lamella.[54,58] This crosshatching morphology manifests itself for most melt crystallization conditions (i.e., between 90 and 160 °C).[58] Examination of the crosshatched morphology by TEM suggests that leading radial lamellae are thicker than the daughter tangential lamellae and do not pack in stacks, except possibly at the highest crystallization temperatures (150 °C and above) in the outer regions of spherulites.[57] Lamellar stacking, when observed by transmission electron microscopy at intermediate crystallization temperatures (120−150 °C), appears to be limited to daughter tangential lamellae and is generally spatially restricted. In view of the difference between daughter and parent lamellae and the difference in their stacking behavior, one should not expect to find simple correlations between the peak melting temperature (characteristic of the thicker radial lamellae) and the lamellar thickness calculated from the SAXS data (most likely dominated by periodic density fluctuations within the stacks of thinner lamellae). Qualitatively, it appears that lamellar thicknesses inferred from the SAXS analysis are much lower than those estimated by transmission electron microscopy.[9,12,57]

Further inconsistencies in the results obtained by SAXS are uncovered when considering recent studies by Ryan et al.[66] Using, simultaneously, calorimetry and synchrotron SAXS/WAXD techniques, they followed the evolution of the invariant, correlation function, and degree of crystallinity of it-PP during isothermal melt crystallization at 133 °C. During primary crystallization, the long spacing obtained either from the correlation function (L_γ) or the Bragg maximum in the Lorentz corrected scattering profile (L_B) is constant. However, in contrast to the SAXS analysis at room temperature by Mezghani et al.[12] where L_B was systematically larger than L_γ by ca. 20%, Ryan's et al.[66] study yields the opposite conclusion (i.e., L_B is lower than L_γ by ca. 20%), suggesting apparent but unexplained differences in long spacing distributions. In the latter study, the lamellar thickness estimated from the correlation function appears to be independent of crystallization time during the primary crystallization stage.[66] This is apparently inconsistent with the suggestion by Mezghani et al.[12] that significant lamellar thickening occurs even during primary crystallization and is at the origin of the increase in the observed melting temperature. For a quantitative assessment of the relationship between lamellar thickening and an increase in observed melting temperature, we have plotted in Figure 14 T_m' versus l data generated with the T_m, σ_e values reported by Cheng et al.[9] and Mezghani et al.[12] and these estimated in this work. We have shown in Figure 2 that, for all crystallization temperatures investigated in this study, the observed melting temperature increases linearly with the logarithm of the crystallization time during primary crystallization. For crystallization temperatures in the range 129−136 °C, the increase in the observed melting temperature during the primary crystallization stage is approximately 1.0−1.5 °C, in agreement with data reported by Mezghani et al.[12] For a crystallization temperature of 133 °C, the long spacing and lamellar thickness estimated by Ryan et al.[66] are approximately 200 and 135 Å, respectively, in qualitative agreement (within 20% or so; see above) with estimates by Mezghani et al.[12] Focusing now in Figure 14, a 1.0−1.5 °C change in the observed melting temperature can arise from a change in the lamellar thickness, the magnitude of which depends only on the magnitude of the σ_e, T_m parameters for α-phase it-PP. If our parameters are used, the predicted change in lamellar thickness is relatively small (3.5−5 Å or so). However, whether Mezghani et al. or Cheng et al.'s values are used, a measurable change in lamellar thickness is expected (Δl = 10 or 25 Å). Since such changes are not observed in Ryan et al.'s data,[66] it suggests an inconsistency in the SAXS/DSC approach. Preliminary AFM studies in our laboratory, to be reported in detail later and aimed at studying the evolution of the lamellar thickness with crystallization time, confirm (1) the relatively small change in the lamellar thickness with the crystallization time and (2) the smaller estimate of the lamellar thickness by SAXS than by microscopy. The fact that lamellar thicknesses obtained by SAXS are underestimated is also confirmed in recent work by White et al.[57]

A final issue related to the use of SAXS to determine lamellar thicknesses pertains to the possibility that samples crystallized at extremely large undercoolings (as in Cheng et al. studies) may contain a nonnegligible

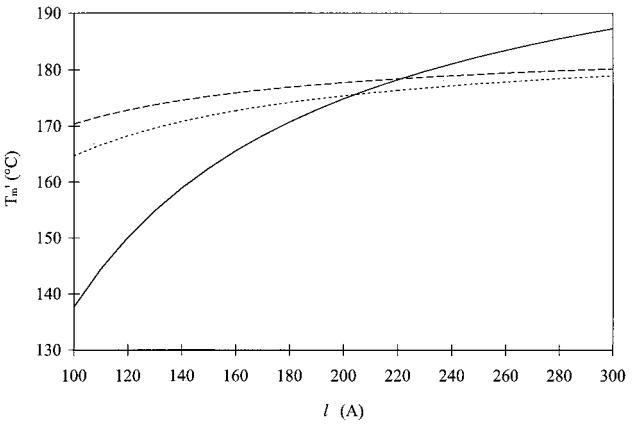

Figure 14. Predicted correlation between the observed melting temperature and lamellar thickness. Full curve (this work); long dashed curve (Cheng et al.[9]); short dashed curve (Mezghani et al.[12]).

fraction of smectic or even β-phase it-PP, which would contribute in some unpredictable fashion to the SAXS profile but are ignored in the calorimetric analysis if one focuses on the endotherm peak position.

It should therefore be apparent from the above discussion that use of the Gibbs−Thomson analysis to infer the equilibrium melting temperature of it-PP has very serious limitations, when it is based on SAXS data. These limitations could obviously be overcome if the thickness of leading radial lamellae are measured through a direct technique such as transmisssion electron microscopy.

Having established a rationale for the lack of accuracy of previous estimates of T_m and σ_e through a combination of SAXS and DSC and for the problems associated with the linear HW approach, we have proposed a different strategy for the evaluation of these thermodynamic quantities. The value of $T_m = 212 \pm 3$ °C appears to be well-established on the basis of the nonlinear HW approach and is consistent with results from the analysis of the temperature dependence of spherulitic growth rates. The new values proposed in this work for the basal plane interfacial free energy, σ_e^1, and the C_2 parameter depend critically on the choice of both T_m and σ. Note that similar estimates of σ were obtained from the Thomas−Staveley empirical relation and the $\sigma-C_\infty$ correlation. It would be, however, more satisfying to obtain independent estimates of σ_e^1 through measurements of the initial lamellar thickness as a function of the crystallization temperature and of σ_{em} through correlations between the lamellar thickness and observed melting temperature, using electron or atomic force microscopy. Such studies are currently in progress and will allow us to probe the validity of the assumptions used in this work and the accuracy of the reported thermodynamic parameters.

For the sake of completeness and rigor, it is also important to note a number of unresolved issues for it-PP crystallization, issues which are clearly pertinent to the above discussion. First, there is still some uncertainty as to the nature of the growth plane for the α-phase of it-PP. Previous analyses of the temperature dependence of the it-PP spherulitic growth rate have universally adopted (110) as the growth plane for this crystal phase. The appropriateness of this choice appears to be supported by electron microscopy studies by Lotz, Wittmann, and co-workers using the decoration method.[67] However, Petraccone et al.[68] suggest on the basis of tacticity and crystallographic considerations that folding must occur in a direction parallel to the (010) plane. If this suggestion is indeed correct, then the folding process would take place along the long axis of it-PP lathlike crystals (i.e., folds would not be parallel to the growth front but perpendicular to it and into the melt). This situation obviously differs dramatically from that addressed by the LH secondary nucleation model,[35,36] and one should not expect the growth rate data to be accounted for by that model. It is, however, fairly difficult to envision how such a process could indeed take place. In a more recent study, Petraccone et al.[69] calculated fold conformational energies for possible folds in it-PP, assuming folding parallel to the (010) plane. The corresponding fold interfacial free energies are found to be in the range of 50−70 erg·cm^{-2}, in accord with estimates derived from the analysis of the temperature dependence of spherulitic growth rates for α-phase it-PP, assuming $T_m = 185$ °C. However, as indicated above, the LH theory should not apply for folding in directions normal to the growth front and a melting temperature of 185 °C is not justifiable.

A second unresolved issue pertains to the multiple melting behaviors observed for Ziegler−Natta it-PP in two different ranges of crystallization temperatures ($T < 120$ °C and $135 < T < 150$ °C).[4,38,39,70−74] The most complete studies suggest that, in both cases, this phenomenon is associated with a melting−recrystallization−remelting process.[71,72] This assertion can certainly be understood at the lowest temperatures, where indeed, initial melting occurs in a temperature range where recrystallization could take place on a short time scale. It is, however, difficult to understand why this process would reappear at relatively high temperatures (135−150 °C), where rates of crystallization appear to be increasingly slower, whereas it is not present in the intermediate temperature range ($120 < T < 135$ °C). It appears more appealing to rationalize the onset of the double melting behavior for samples crystallized in the higher temperature range in terms of a bimodal distribution of lamellar thicknesses (thicker dominant radial lamellae and thinner tangential or radial daughter lamellae). Indeed, as shown by White et al.,[57] for crystallization temperatures below ca. 130 °C, the difference in thickness between dominant and crosshatching lamellae becomes vanishingly small, whereas at higher temperatures (ca. 140 °C) the thickness of these lamellae differ more significantly, which should lead to separate and easily resolvable melting endotherms. As the temperature of crystallization is raised further (ca. 150−160 °C), the population of crosshatching lamellae decreases significantly, which should lead again to a single melting endotherm, as observed experimentally.[72−74] We do not reject the possibility that melting−recrystallization occurs to a limited extent upon heating, especially at the lowest heating rates. It is, however, unlikely, especially in view of the recrystallization rates reported in the literature[72] and the known existence of a bimodal distribution of lamellar thicknesses,[57] that the double melting behavior be entirely attributed to a melting−recrystallization process. This issue, certainly, deserves further attention.

On a related matter, the existence of two limiting structures have been proposed for the α-form.[75−77] The α_2-structure is an ordered limiting structure (crystallographic symmetry $P2_1/c$) with a well-defined arrangement of up and down 3_1 helices, whereas the α_1-structure is a disordered limiting structure (crystallographic symmetry $C2/c$) with a random distribution of up and down helices. Guerra et al.[78] showed on the basis of diffraction studies that structures more akin to the α_2-form are favored at high annealing temperatures ($T_a \gg 153$ °C). Using complementary calorimetric studies, they inferred from the observation of single endotherms in the thermogram of annealed samples that the annealing process at a high temperature leads to a "continuum" of structures intermediate between the α_1- and the α_2-forms. It is concluded from their study that annealing below 153 °C should not yield wildly different crystal structures. From this observation, it would be tempting to conclude that the spherulitic growth rates reported in this manuscript (measured from 123 to 154 °C) can be safely analyzed in the context of a single crystalline phase. It is, however, not known at this time how the result of these annealing studies can be applied to the case of isothermal crystallization.

Recent studies by Awya[79] suggest that isothermal melt crystallization at 155 °C of a low molecular weight it-PP results in a predominantly α_2 crystal form. Furthermore, significant melting−recrystallization effects would hamper our ability to correlate crystallization and melting temperatures. Recrystallization during heating would lead to the formation of the more ordered structure, which is likely to have a slightly different equilibrium melting temperature than that of the initial disordered limiting structure.[80] While these issues cannot be resolved with currently available information, they certainly place some limitations on the claims that are made in the present manuscript. It is, nevertheless, anticipated that future examinations of the correlation between the crystallization temperature, melting temperature, and lamellar thickness can shed some light on the validity of the assumptions used in this manuscript and on how serious the above limitations truly are.

Conclusions

In this manuscript, we have applied a new strategy for the evaluation of the thermodynamic parameters relevant for crystal growth and melting processes in the case of it-PP prepared by Ziegler−Natta catalysts. The reliability of our method is strictly dependent on (1) the applicability of the classical relationship between the initial lamellar thickness and undercooling ($l = 2\sigma_e^1/\Delta G_f + C_2$), (2) the assumption that σ_e^1 can be equated to σ_{em}, and (3) the appropriateness of the method used to estimate melting temperatures of initial (i.e., nonthickened) lamellae. We proposed that, for it-PP, the values of $T_m = 212 \pm 3$ °C, $\sigma_e = 146 \pm 48$ erg·cm^{-2}, and $C_2 = 52 \pm 17$ Å are more consistent with the limited direct morphological data available in the literature than these previously reported on the basis of a linear HW approach or of the SAXS-based Gibbs−Thomson analysis. We emphasized the central importance of an accurate estimation of the equilibrium melting temperature in the analysis of crystal growth rate data and in a rigorous test of the Lauritzen−Hoffman surface nucleation model. Possible limitations of the current approach for the case of isotactic polypropylene have been discussed. Further possible refinement of the magnitude of the basal plane interfacial free energy, σ_e^1, and the C_2 parameter must await more complete morphological studies of it-PP. The results of such studies can in turn provide an evaluation of the self-consistency of the LH theory.

Acknowledgment. Support of this research by the National Science Foundation through the NSF Young Investigator Program (DMR 93-57512) is greatfully acknowledged. Donation of the it-PP sample by Exxon Chemical was greatly appreciated. We also wish to gratefully acknowledge stimulating discussions of this work with Drs. J. D. Hoffman and M. Mansfield.

References and Notes

(1) Marand, H.; Xu, J.; Srinivas, S. *Macromolecules* **1998**, *31*, 8219.
(2) Wyckoff, H. W. *J. Polym. Sci.* **1962**, *62*, 83.
(3) Danusso, F.; Gianotti, G. *Makromol. Chem.* **1964**, *80*, 1.
(4) Samuels, R. J. *J. Polym. Sci., Polym. Phys. Ed.* **1975**, *13*, 1417.
(5) Martuscelli, E.; Pracella, M.; Zambelli, A. *J. Polym. Sci., Polym. Phys. Ed.* **1980**, *18*, 619.
(6) Miller, R. L.; Seeley, E. G. *J. Polym. Sci., Polym. Phys. Ed.* **1982**, *20*, 2297.
(7) Martuscelli, E.; Pracella, M.; Crispino, L. *Polymer* **1983**, *24*, 693.
(8) Monasse, B.; Haudin, J. M. *Colloid Polym. Sci.* **1985**, *263*, 822.
(9) Cheng, S. Z. D.; Janimak, J. J.; Zhang, A.; Cheng, H. N. *Macromolecules* **1990**, *23*, 298.
(10) Cheng, S. Z. D.; Janimak, J. J.; Zhang, A.; Hsieh, E. T. *Polymer* **1991**, *32*, 648.
(11) Mezhgani, K.; Phillips, P. J. *Macromolecules* **1994**, *27*, 6145.
(12) Mezghani, K.; Campbell, R. A.; Phillips, P. J. *Macromolecules* **1994**, *27*, 997.
(13) Falkai, B. V. *Makromol. Chem.* **1960**, *41*, 86.
(14) Rybnikar, F. *Collect. Czech. Chem. Commun.* **1962**, *28*, 320.
(15) Cox, W. W.; Duswalt, A. A. *Polym. Eng. Sci.* **1967**, *10*, 309.
(16) Kamide, K.; Toyama, K. *Kobunshi Kagaku* **1969**, *25*, 49.
(17) Fatou, J. G. *Eur. Polym. J.* **1971**, *7*, 1057.
(18) Mucha, M. *J. Polym. Sci., Polym. Symp.* **1981**, *69*, 79.
(19) Yadav, Y. S.; Jain, P. C. *Polymer* **1986**, *27*, 721.
(20) Falkai, B. V.; Stuart, H. A. *Kolloid Z.* **1959**, *162*, 309.
(21) Falkai, B. V.; Stuart, H. A. *Makromol. Chem.* **1960**, *41*, 86.
(22) Binsbergen, F. L.; DeLange, B. G. M. *Polymer* **1970**, *11*, 309.
(23) Lovinger, A. J.; Chua, J. Q.; Gryte, C. C. *J. Polym. Sci., Polym. Phys. Ed.* **1977**, *15*, 641.
(24) Goldfarb, L. *Makromol. Chem.* **1978**, *179*, 2297.
(25) Wlochowicz, A.; Eder, M. *Polymer* **1981**, 22, 1285.
(26) Martuscelli, E.; Silvestre, C.; Abate, G. *Polymer* **1982**, *23*, 229.
(27) Clark, E. J.; Hoffman, J. D. *Macromolecules* **1984**, *17*, 878.
(28) Janimak, J. J.; Cheng, S. Z. D. *Polym. Bull.* **1989**, *22*, 95.
(29) Pospisil, L.; Rybnikar, F. *Polymer* **1990**, *31*, 477.
(30) Okada, T.; Saito, H.; Inoue, T. *Macromolecules* **1992**, *25*, 1908.
(31) Celli, A.; Fichera, A.; Marega, C.; Marigo, A.; Paganetto, G.; Zannetti, R. *Eur. Polym. J.* **1993**, *29*, 1037.
(32) Wang, Y. F.; Lloyd, D. R. *Polymer* **1993**, *34*, 2324.
(33) Ding, Z.; Spruiell, J. E. *J. Polym. Sci., Polym. Phys. Ed.* **1997**, *35*, 1077.
(34) Hoffman, J. D.; Weeks, J. J. *J. Res. Natl. Bur. Stand. (U.S.)* **1962**, *A66*, 13.
(35) Hoffman, J. D.; Davis, G. T.; Lauritzen, J. I. In *Treatise on Solid State Chemistry*; Hannay, N. B., Ed.; Plenum Press: New York, 1976; Vol. 3, Chapter 7.
(36) Hoffman, J. D.; Miller, R. L. *Polymer* **1997**, *38*, 3151.
(37) Point, J.-J.; Janimak, J. J. *J. Cryst. Growth* **1993**, *131*, 501.
(38) Kamide, K.; Yamaguchi, K. *Makromol. Chem.* **1972**, *162*, 205.
(39) Kamide, K.; Yamaguchi, K. *Makromol. Chem.* **1972**, *162*, 219.
(40) Plazek, D. L.; Plazek, D. J. *Macromolecules* **1983**, *16*, 1469.
(41) Pearson, D. S.; Fetters, L. J.; Younghouse, L. B.; Mays, J. W. *Macromolecules* **1988**, *21*, 478.
(42) Huang, J.; Prasad, A.; Marand, H. *Polymer* **1994**, *35*, 1896.
(43) Huang, J.; Marand, H. *Macromolecules* **1997**, *30*, 1069.
(44) Marand, H.; Hoffman, J. D. *Macromolecules* **1990**, *23*, 3682.
(45) Snyder, C. R.; Marand, H.; Mansfield, M. *Macromolecules* **1996**, *29*, 7508.
(46) Snyder, C. R.; Marand, H. *Macromolecules* **1997**, *30*, 2759.
(47) Iler, H. D. Ph.D. Dissertation, Virginia Polytechnic Institute and State University, Blacksburg, VA, 1996.
(48) Marand, H.; Iler, H. D.; Snyder, C. R. *Bull. Am. Phys. Soc.* **1996**, *41* (1), 394.
(49) Thomas, D. G.; Staveley, L. A. K. *J. Chem. Soc.* **1952**, 4569.
(50) See: Hoffman, J. D.; Miller, R. L.; Marand, H.; Roitman, D. B. *Macromolecules* **1992**, *25*, 2221. On the basis of neutron scattering experiments, the characteristic ratio of it-PP and at-PP are found to be identical ($C_\infty = 6.0$) (see: Xu et al. *Adv. Polym. Sci.* **1995**, *120*, 1 and Fetters et al. *Macromolecules* **1993**, *27*, 4639).
(51) Khoury, F. A. *J. Res. Natl. Bur. Stand. (U.S.)* **1966**, *70A*, 29.
(52) Binsbergen, F. L.; de Lange, B. G. M. *Polymer* **1968**, *9*, 23.
(53) Padden, F.; Keith, H. D. *J. Appl. Phys.* **1973**, *44*, 1217.
(54) Wittmann, J. C.; Lotz, B. *J. Polym. Sci., Polym. Phys. Ed.* **1985**, *23*, 205.
(55) Norton, D. R.; Keller, A. *Polymer* **1985**, *26*, 704.
(56) Olley, R. H.; Bassett, D. C. *Polymer* **1989**, *30*, 399.
(57) White, H. M.; Bassett, D. C. *Polymer* **1997**, *38*, 5515.
(58) Lotz, B.; Wittmann, J. C.; Lovinger, A. J. *Polymer* **1996**, *37*, 4979.
(59) McCrum, N. G. *Polymer* **1984**, *25*, 299.
(60) Boyd, R. H. *Polymer* **1985**, *26*, 1123.
(61) Syi, J.-L.; Mansfield, M. *Polymer* **1988**, *29*, 987.
(62) Schaefer, D.; Spiess, H. W.; Suter, U. W.; Fleming, W. W. *Macromolecules* **1990**, *23*, 3431.
(63) Skinner, J. L.; Park, Y. H. *Macromolecules* **1984**, *17*, 1735.

(64) VanderHart, D. L.; Alamo, R. G.; Kim, M. H.; Mandelkern, L.; Perez, E.; Mansel, S. *Bull. Am. Phys. Soc.* **1998**, *43*, 270.
(65) Albrecht, T.; Strobl, G. *Macromolecules* **1995**, *28*, 5267.
(66) Ryan, A. J.; Stanford, J. L.; Bras, W.; Nye, T. M. W. *Polymer* **1997**, *38*, 759.
(67) Lotz, B.; Graff, S.; Wittmann, J. C. *J. Polym. Sci., Polym. Phys. Ed.* **1985**, *24*, 2017.
(68) Petraccone, V.; Pirozzi, B.; Meille, S. V. *Polymer* **1986**, *27*, 1665.
(69) Petraccone, V.; Pirozzi, B.; Meille, S. V. *Eur. Polym. J.* **1989**, *25*, 43.
(70) Corradini, P.; Napolitano, R.; Oliva, L.; Petraccone, V.; Pirozzi, B. *Makromol. Chem., Rapid Commun.* **1982**, *3*, 753.
(71) Carfagna, C.; De Rosa, C.; Guerra, G.; Petraccone, V. *Polymer* **1984**, *25*, 1462.
(72) Petraccone, V.; De Rosa, C.; Guerra, G.; Tuzi, A. *Makromol. Chem., Rapid Commun.* **1984**, *5*, 631.
(73) Petraccone, V.; Guerra, G.; DeRosa, C.; Tuzi, A. *Macromolecules* **1985**, *18*, 813.
(74) Passingham, C.; Hendra, P. J.; Cudby, M. E. A.; Zichy, V.; Weller, M. *Eur. Polym. J.* **1990**, *26*, 631.
(75) Natta, G.; Pino, P.; Corradini, P.; Danusso, F.; Mantica, E.; Mazzanti, G.; Moraglio, G. *J. Am. Chem. Soc.* **1952**, *77*, 1708.
(76) Mencik, Z. *J. Macromol. Sci. Phys.* **1972**, *B6*, 101.
(77) Hikosaka, M.; Seto, T. *Polym. J.* **1973**, *5*, 111.
(78) Guerra, G.; Petraccone, V.; Corradini, P.; De Rosa, C.; Napolitano, R.; Pirozzi, B.; Giunchi, G. *J. Polym. Sci., Polym. Phys. Ed.* **1984**, *22*, 1029.
(79) Awaya, H. *Polymer* **1988**, *29*, 591.
(80) On the basis of energy calculations, the $P2_1/c$ structure appears slightly more stable than the $C2/c$ structure (Corradini, P.; Petraccone, V.; Pirozzi, B. *Eur. Polym. J.* **1983**, *19*, 299).
(81) Bu, H.-S.; Cheng, S. Z. D.; Wunderlich, B. *Makromol. Chem., Rapid Commun.* **1988**, *9*, 76.

MA980748Q